Flow Patterns of Liquids in a Cylindrical Mixing Vessel with Baffles

By

Shinji Nagata, Kazuo Yamamoto, Kenji Hashimoto
and Yūji Naruse*

(Received April 30, 1959)

The velocity distribution of a liquid in a cylindrical mixing vessel with flat-plate-baffles was measured by a method similar to that adopted in the case without baffles[1].

Some of the experimental results are shown in **Figs. 3, 4, 5, 6, 7, 8** and **9**.

Variations of the liquid velocity distribution caused by inserting baffle-plates are shown in **Fig. 10**. Obviously, the insertion of baffle-plates reduces the circulation flow around the impeller axis (the tangential component v_t of liquid velocity) and increases the circulation flow in the vertical direction.

The discharging performance of various impellers is represented by the ratio N_{p_B}/N_{q_1}, which is the dimensionless factor corresponding to the relative power required for the unit quantity of discharge. The comparisons of these ratios for various impellers are shown in **Table 3**, together with those for the non-baffled condition. It is to be noted that, in spite of a considerable increase in N_{q_1}, the circulation efficiency of the agitators is eventually lowered by inserting baffle-plates.

Furthermore, the power consumption in the neighbourhood of the impeller ($N_{p_{ipm}}$) was calculated and compared with that consumed in the outer region of the vessel (ΔN_p) as shown in **Table 4**,

It may be considered that the improvement in the circulating capacity is accomplished by the proper design of the baffle-plates.

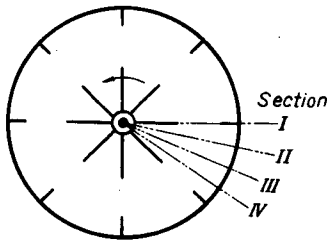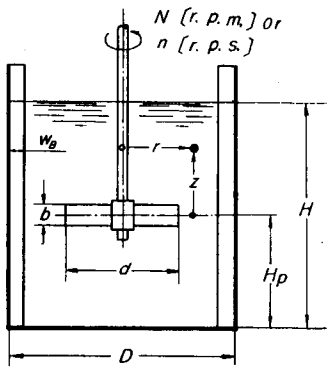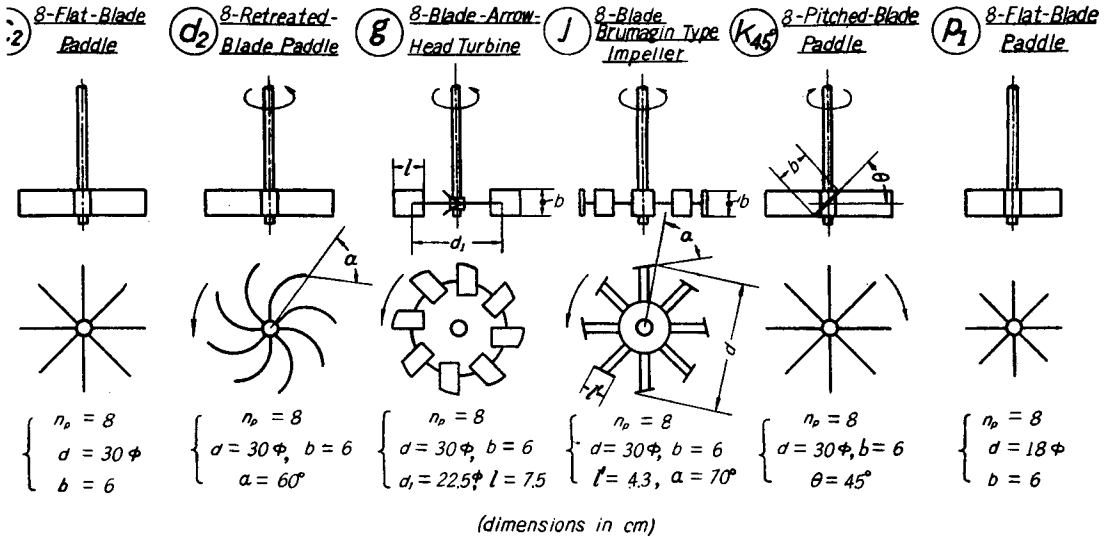## I. Equipment Used and Method of Measurement

1) Impellers and Vessel

The impellers used are shown in **Table 1** and the conditions of their installation are shown in **Fig. 1**. The mixing vessel used is the same as in the previous report except that baffle-plates are inserted. It has a diameter of 58.5 cm and is filled with tap water to a depth equal to the diameter. Eight flat-plate-baffles 4.5 cm wide are used as those which correspond to the so-called fully-baffled condition[2]. Those baffle plates were installed along the circumference of the tank wall at equal distances and extended to the bottom of the vessel.

By the insertion of so many baffle-plates, the flow pattern of the liquid in the

---

* Department of Chemical Engineering

Table I   Various Types of Impellers used

$\overline{2}$ 8-Flat-Blade Paddle	d_2 8-Retreated- Blade Paddle	g 8-Blade-Arrow- Head Turbine	J 8-Blade Brumagin Type Impeller	K_{45} 8-Pitched-Blade Paddle	P_1 8-Flat-Blade Paddle

$\begin{cases} n_p = 8 \\ d = 30\,\phi \\ b = 6 \end{cases}$ $\begin{cases} n_p = 8 \\ d = 30\,\phi,\ b = 6 \\ a = 60° \end{cases}$ $\begin{cases} n_p = 8 \\ d = 30\,\phi,\ b = 6 \\ d_1 = 22.5\phi,\ l = 7.5 \end{cases}$ $\begin{cases} n_p = 8 \\ d = 30\,\phi,\ b = 6 \\ l = 4.3,\ a = 70° \end{cases}$ $\begin{cases} n_p = 8 \\ d = 30\,\phi,\ b = 6 \\ \theta = 45° \end{cases}$ $\begin{cases} n_p = 8 \\ d = 18\,\phi \\ b = 6 \end{cases}$

(dimensions in cm)

$D = 58.5^{cm\phi}$

$H = D,\qquad H_p = H/2$

$w_\theta = 4.5^{cm},\qquad n_\theta = 8$

Fig. 1. Schematic Diagram of Impeller and Vessel (Fully-Baffled Type).

agitated vessel was considerably unified, but it did not yet have axial symmetry with respect to the agitator axis. Therefore the discharging flow pattern was measured at the several vertical sections passing through the agitator axis as shown in **Fig. 1** (Section I∼IV). The measurement was limited to the upper half of the liquid depth ($z \geq 0$), because the flow had practically plane symmetry with respect to the rotation plane of the impellers. Although it might be necessary to obtain more rigorous confirmation of this conclusion in the future, it was generally confirmed by the optical observation of flow except in the neighbourhood of the tank bottom and the liquid surface. The optical method is similar to that used by J. P. Sachs and J. H. Rushton, that is, a plane beam of light is projected through a vertical section of the agitated liquid containing suspended particles. Photographs of the trajectory of the gleaming particles, for example naphthalene powder, show the approximate flow pattern. **Phot. 1∼3** are some examples.

2) Equipment for Measurements

Details of the pitot-tube and its accessories used for the measurement of the flow are omitted in this report, since they are similar to those shown in the previous report[1] with the exception of some improvements. In the case of the baffled condition, circulation around the agitator-axis is remarkably reduced and the vertical circulation becomes predominant as is discussed later. Thus the three dimensional flow directions should be detected by measuring the angles θ' and φ' as shown in **Fig. 2.** That is the main difference from the previous report. The measurement of the resultant velocity V, is just the same as in the previous report. The flow pattern for the baffled condition is so complicated that the reliability of the data obtained seems to be lower than that for the non-baffled condition.

3) Method for Calculation of the Three Components of the Lipuid Velocity

The three components of liquid velocity, i.e., (1) radial velocity v_r, (2) tangential (or circumferential) velocity v_t and (3) axial (or vertical) velocity v_z are shown in **Fig. 2 (c)**, and these are calculated from the values of θ', φ' and V using the following equations:

Fig. 2. Measurement of Flow Direction.

$$\left.\begin{aligned}
v_r &= V/\sqrt{(1+\tan^2\theta'+\tan^2\varphi')} \\
v_t &= V\cdot\tan\theta'/\sqrt{(1+\tan^2\theta'+\tan^2\varphi')} \quad \text{or} \quad v_t = v_r\tan\theta' \\
v_z &= V\cdot\tan\varphi'/\sqrt{(1+\tan^2\theta'+\tan^2\varphi')} \quad \text{or} \quad v_z = v_r\tan\varphi'
\end{aligned}\right\} \quad (1)$$

and the resultant velocity v on the $r-z$ plane is also calculated by the equation:

$$v = V\cdot\sqrt{(1+\tan^2\varphi')}/\sqrt{(1+\tan^2\theta'+\tan^2\varphi')}\,. \qquad (2)$$

The angle between the direction of v and the horizontal plane is equal to φ'.
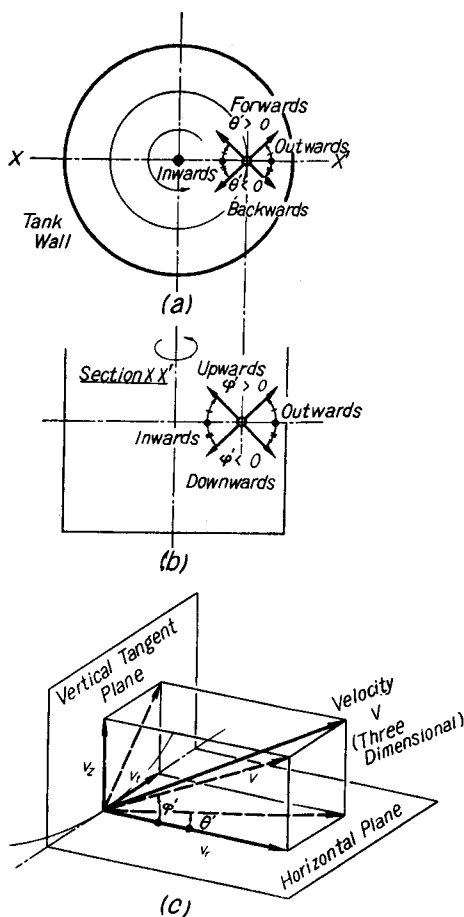
II. Results

As typical examples of θ', φ' and V, the data obtained on section IV in the case of an 8–flat-blade paddle (refer to **Table 1** (c_2)) are shown in **Figs. 3, 4** and **5**. In **Fig. 3,** the distribution of the angle θ' at various heights is drawn for several radial positions. **Fig. 4** and **Fig. 5,** show the distribution of angle φ' and the resultant velocity V in various radial positions for several horizontal levels respectively. These results are so complicated that it is difficult to understand the flow pattern of the liquid intuitively. From these data, the three components of liquid velocity v_r, v_t and v_z are calculated using Eq. (1)
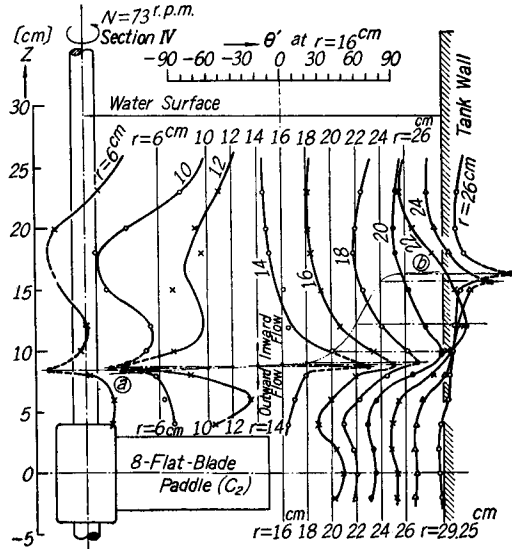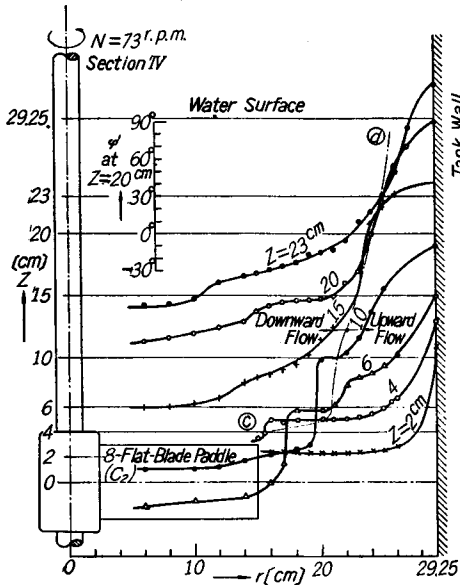
Fig. 3. Distribution of θ' for 8–Flat-Blade Paddle.

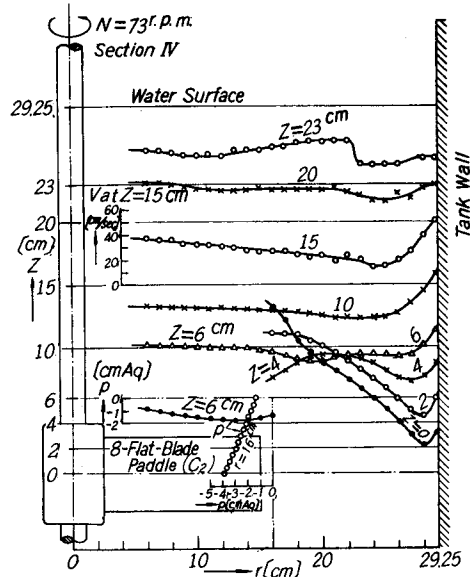Fig. 4. Distribution of φ' for 8–Flat-Blade Paddle,

Fig. 5. Distribution of Resultant Velocity V and Static Pressure p for 8–Flat-Blade Paddle,
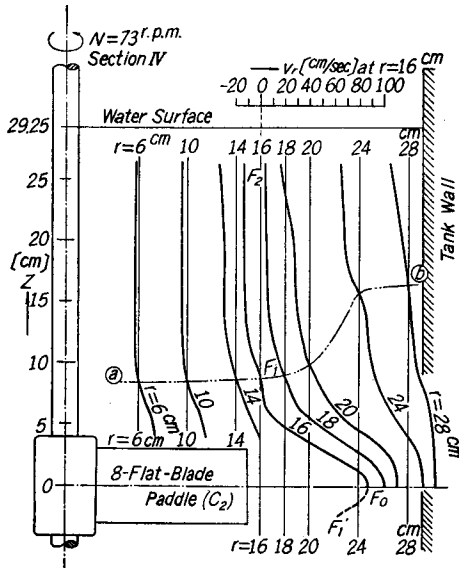
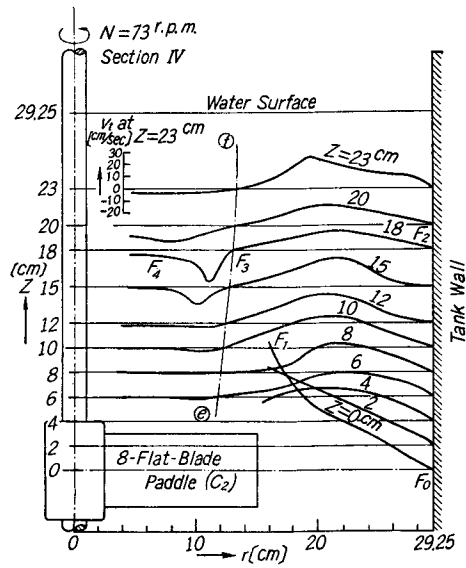Fig. 6. Distribution of Radial Velocity v_r for 8–Flat-Blade Paddle.

Fig. 7. Distribution of Tangential Velocity v_t for 8–Flat-Blade Paddle.

and, consequently **Figs. 6, 7** and **8** are drawn. To explain more precisely about **Fig. 6,** the distribution of the radial component of liquid velocity v_r at various levels is drawn for several radial positions and its positive or negative value corresponds to the outward or inward flow respectively. The two dotted-chain-line (a)—(b) is the border-line between the inward- and outward-flow. For instance, the outward flow discharged from the neighbourhood of the impeller blades (F_1 F_0 F_1') changes its direction due to the vessel wall and the baffle plates and changes into the inward flow (F_1 F_2) in the upper region. The width of the outward flow is much wider than that of the impeller blades.

Fig. 8. Distribution of Axial Velocity v_z for 8–Flat-Blade Paddle.

In **Fig. 7,** the circumferential velocity distribution (v_t) in various radial positions is drawn for several horizontal levels. The magnitude of v_t is rather low except in the vicinity of the impeller (e.g. F_0F_1 is the distribution of v_t at the impeller level). It
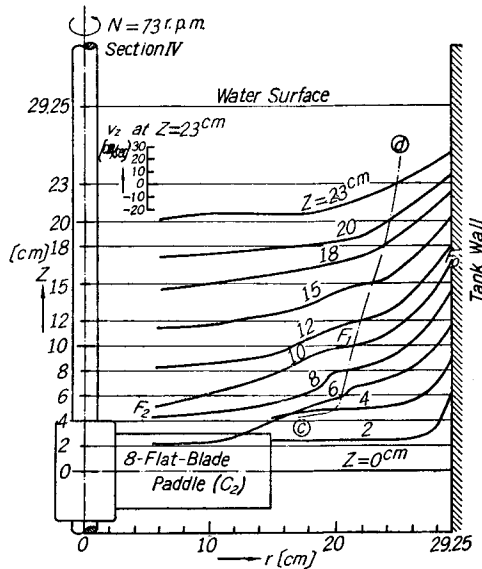
is to be noted that there is a counter flow $(v_t < 0)$ in the central part, and even a sharp counter current $(F_3 \, F_4)$ here and there, in the neighbourhood of the agitator axis. That is because strong eddies occur locally, as will be explained later. In **Fig. 8,** the distribution of the vertical component of the liquid velocity v_z in various radial positions is drawn for several horizontal levels. The chain-line (c)—(d) is the border-line between upward- and downward- flow and upward flow occurs in the outer region of the line and downward flow in the inner region.

In short, except in the vicinity of the impellers, the circumferential velocity v_t, being impeded by the baffle plates, is no longer the main flow and the circulation flow in the vertical direction becomes pre-dominant. In other words, the discharging flow from the neighbourhood of the tip of the blades, colliding with the tank wall, turns upwards (or downwards in the region below the impeller — the same statement will be omitted hereafter), and then turns downwards in the central region of the vessel until it is finally sucked into the impeller again. **Fig. 9** shows the flow pattern on the section IV, which is obtained by calculating v and φ' from the data of **Figs. 3, 4** and **5** using Eq. (2). In this diagram, point V is the intersection of the

Fig. 9. Flow Pattern of Circulation Flow for 8–Flat-Blade Paddle.

two dotted-chain-line (a)—(b) and the one dotted chain-line (c)—(d) and shows the center of the vertical circulation. However, the position of the center is not only shifting up and down at each section, but also continually fluctuating all the time, that is, the flow parttern of the vertical circulation is neither stable nor stationary. These phenomena are, as will be explained in the next secttion, caused by the big and strong eddies that are continually generated and dissipated in the liquid by means of the baffle plates.

Since the diagrams of the flow pattern created by any type of impeller is more or less similar as long as the flat-plate baffles are used, other diagrams are omitted. In the next section, the authors intend to compare the discharging performance of several impellers with and without baffle-plates.

III. Comparison of the Results Obtained

1) Variations of the Flow Pattern Caused by the Insertion of Baffle-plates.

Comparisons of the velocity distributions under non-baffled and fully-baffled con-
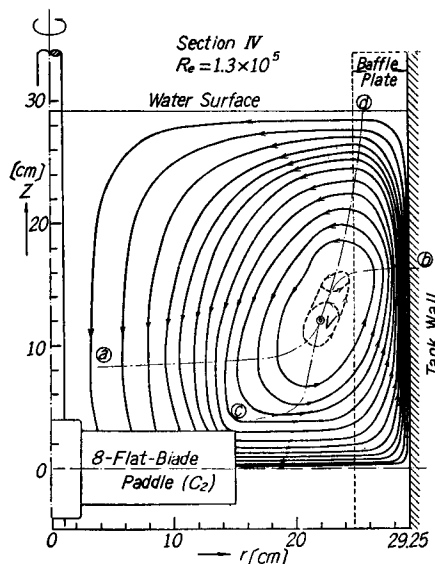
ditions were made as shown in **Fig. 10,** holding other conditions constant, i.e., the impeller (8–flat-blade paddle (c_2)), liquid volume, installation condition of the impeller, agitator speed etc. were the same in both cases. The radial velocity (v_r) distribution at various heights for the radial position $r =$ 16 cm., the circumferential velocity (v_t) distribution and vertical velocity (v_z) distribution at various radial positions for a 15 cm height are compared in **Fig. 10,** with full lines for baffled agitation and broken lines for non-baffled agitation. Obviously, the insertion of the baffle-plates impedes the circumferential flow and increases the

Fig. 10. Variation of Velocity Distribution (on Section IV) by Inserting Baffle Plates.

vertical flow. Also, comparing the discharge flow from the tip of blades F_0F_1 and $F_0''F_1''$, it is obvious that the insertion of baffle-plates increases both the flow velocity and the width of the discharge flow, as though the effective width of the impeller blades were increased. Therefore, the total quantity of vertical circulation would be increased 2-4 times, as will be mentioned later. Furthermore, comparing the flow pattern of baffled agitation (**Fig. 9**) with that of non-baffled agitation (refer to the previous report[1)]), it seems that the distribution of the stream-line is considerably unified by the insertion of baffle-plates. No general statement can be presented about the change of the resultant velocity V, but, on the whole, there is a considerable decrease in V by the insertion of baffle-plates. Anyhow, it may be clear that the insertion of baffle-plates causes important changes upon the mixing characteristics of agitators.

Speaking in great detail, it was ascertcined by optical observation that the actual flow of the agitated liquid would repeat continual and complicated changes with time. **Fig. 11** is a schematic diagram showing the variation and shift of the vortex formation. Four baffle-plates are used for the sake of convenience of taking a photograph. **Fig. 11 (a)** is a diagram showing the positions of the vertical sections to be examined. Sections I, II, III, IV and V were examined in turn. The discharge flow from the tip of the blades collides with the tank wall and the baffle-plate (2), and then forms a circulation having its center at the points V and V', as shown in **Fig. 11 (e)**. As
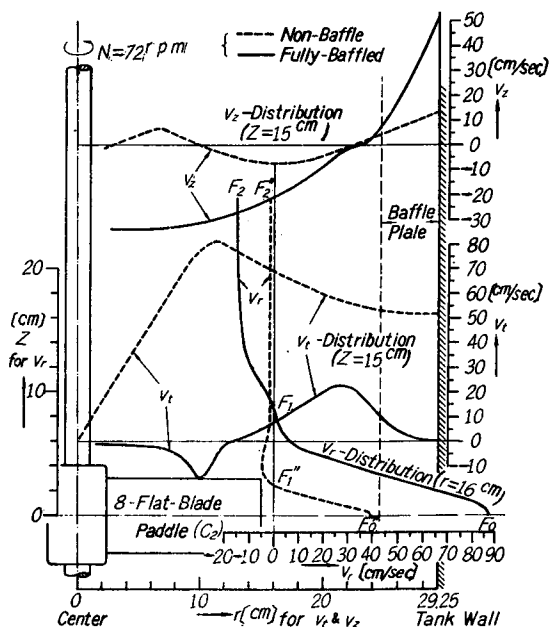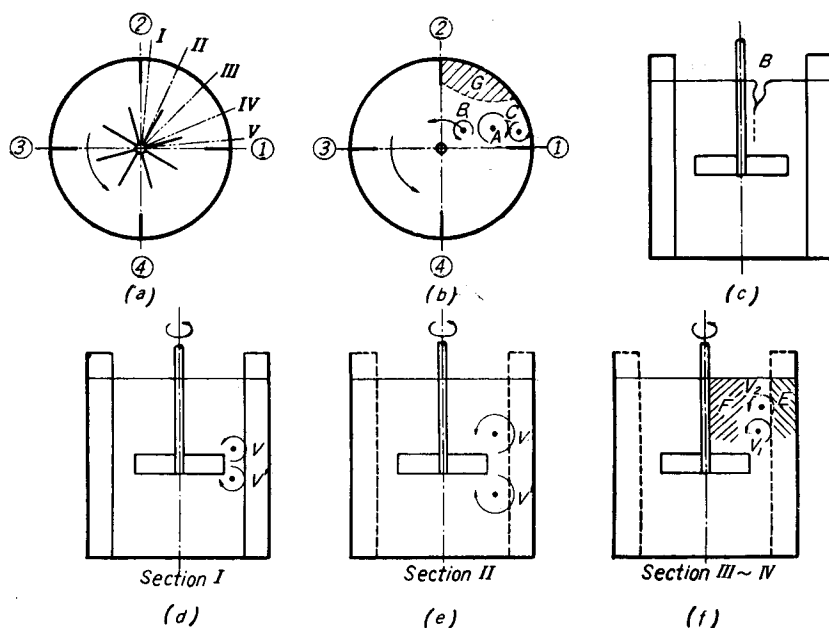
Fig. 11. Schematic Diagram of Vortex Formation in the Mixing Vessel with Baffles.

the section in question is shifted from I to II, III, IV and V, the center of the circulation V also shifts gradually from a point near the tip of blades to a higher position and its flow pattern becomes more and more obscure and unstable. On sections III an IV, the circulation becomes much more unstable and the center of the eddy wanders from V_1 to V_2 continually and sometimes two eddies appear at V_1 and V_2 at the same time (Refer to **Fig. 11 (f)**). The flow pattern shown in **Fig. 9** corresponds to this state of flow. The flow pattern in the central part of the circulation, which is shown by broken-lines in **Fig. 9,** can hardly be made clear. Furthermore, on section V, such a trend becomes so intense, that regular circulation can no longer be observed. **Phot. 1~3** show a few example of those flow patterns. Concerning the circumferential flow, there is a con-current with the rotation of the impellers in the region of E in **Fig. 11 (f),** and a counter-current flow in the region !F. These phenomena are also shown on the diagram of **Fig. 7.** There is a con-current flow $(v_t > 0)$ in F_2F_3 and a counter-current flow $(v_t < 0)$ in F_3F_4. **Fig. 11 (b)** shows the state of eddies on the liquid surface of the vessel. Since the discharge flow from the tip of the blades collides with the baffle-plates (1), a large and comparatively stable cylindrical eddy A is generated and thereafter, small eddies B and C are induced. Eddy C is easily destroyed, because it is very small and weak, but eddy B is considerably stronger, though not stable, and has a tendency to rotate slowly around the agitator
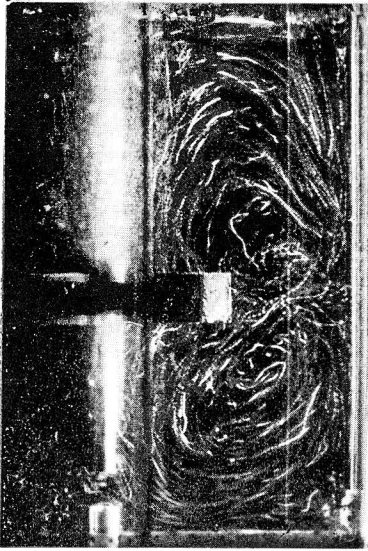
Phot. 1.   Flow Pattern on the Section I
as shown in Fig. 11 (d).
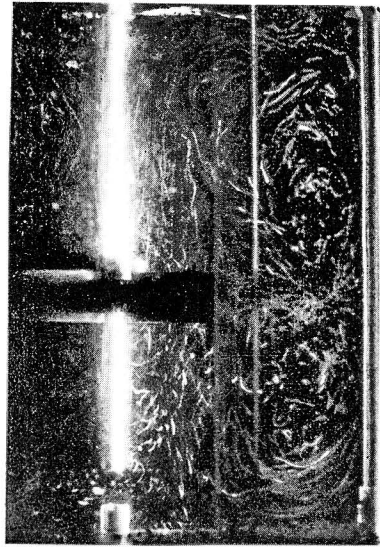
Phot. 2.   Flow Pattern on the Section II
as shown in Fig. 11 (e).
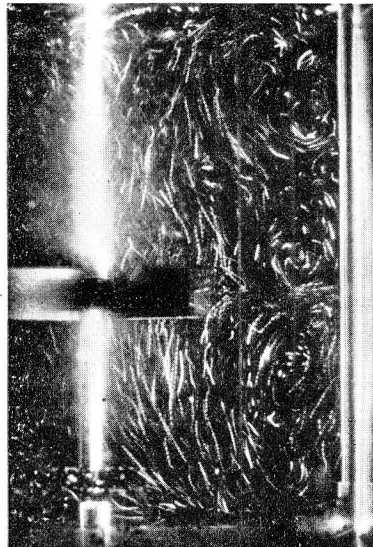
Phot. 3.   Flow Pattern on the Section III
as shown in Fig. 11 (f).

Two eddies are observed in the upper region of the impeller.

axis. Eddies B generated by the neighbouring baffle-plates join into a strong eddy, which forms a hollow vortex on the liquid surface and often sucks air bubbles. The counter-current F in **Fig. 11 (f)** which is shown by F_3F_4 in **Fig. 7** is caused by this strong eddy B. Intermittently, there are some periods during which all of the eddies A, B and C almost disappear. In the region G in **Fig. 11 (b)**, there is a strong upward flow caused by the circulation V as shown in **Fig. 11 (e)**.

2) Comparison of the Discharging and Circulating Performance.

As shown in the previous report, let the discharge flow rate q_1 from the tip of the impeller blades and the flow rate q_2 due to vertical circulation be considered. The coefficient of discharge $N_{q_1}=q_1/nd^3$ and the coefficient of circulation $N_{q_2}=q_2/nd^3$ are also taken up for generalization. Since the flow pattern does not have axial symmetry with respect to the agitator axis, as stated above, they must be measured at each section I~IV respectively, as shown in **Fig. 1**. Thus, if the velocity distribution on a vertical section x is made clear as shown in **Fig. 12**, the following quantity can be defined on the surface of B″C″
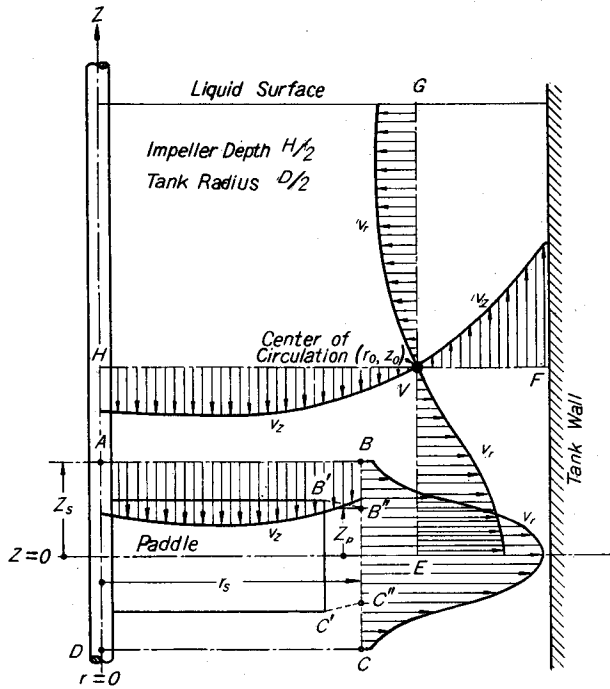
$2r_s = 32^{cm}$, $2Z_s = 12^{cm}$ for the case of energy dissipation

Fig. 12. Schematic Diagram of Circulation and Energy Dissipation.

$$q_{1x} = 4\pi r_s \int_0^{Z_p} v_r dz \qquad (3)$$

where Z_p is the height at which the stream-line passing through the upper corner B′ of the impeller blades intersects the vertical line at the radial position r_s. It is also similar with C′C″.

The following quantities are also defined on the surface EV, FV, GV and HV :

$$\begin{aligned}
q_{2x} &= 4\pi r_0 \int_0^{Z_0} v_r dz = 4\pi \int_{r_0}^{D} v_z r dr \\
&= 4\pi r_0 \int_{Z_0}^{H/2} v_r dz = 4\pi \int_0^{r_0} v_z r dr
\end{aligned} \right\} \qquad (4)$$

Values of q_{1I}, q_{1II}, q_{1III} and q_{1IV} or q_{2I}, q_{2II}, q_{2III} and q_{2IV} are calculated by using Eq. (3) or (4) from the data of the flow pattern on the section I, II, III and IV ; then their average value is taken as the discharge flow rate q_1 or the circulating flow rate q_2, respectively. **Fig. 13** shows the comparison of profiles and rates of the discharge flow at various sections. It is obvious that there is only a small difference in the velocity profiles and the discharge flow rates at the various sections. In this diagram, the distribution of φ' is not shown because it has little effect on the values of the discharge flow rate. Therefore, considering the accuracy of this experiment, it may be adequate to assume that the average value of q_{1I}, q_{1II}, q_{1III} and q_{1IV} is equal to the discharge flow rate q_1. In **Fig. 14,** the profiles of the discharge flow are shown
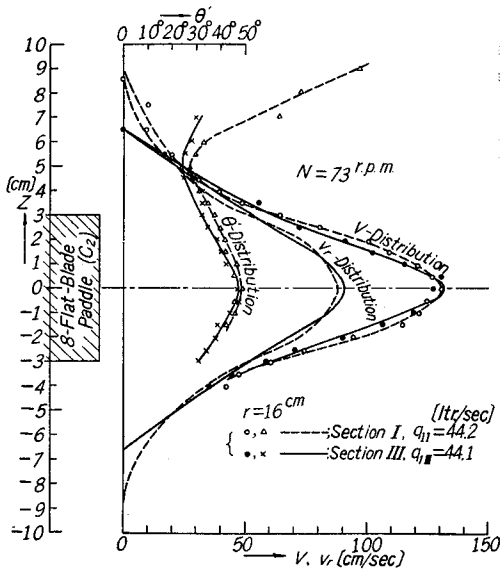
Fig. 13. Velocity Profiles of Discharge Flow at
Various Sections for 8–Flat-Blade Paddle.
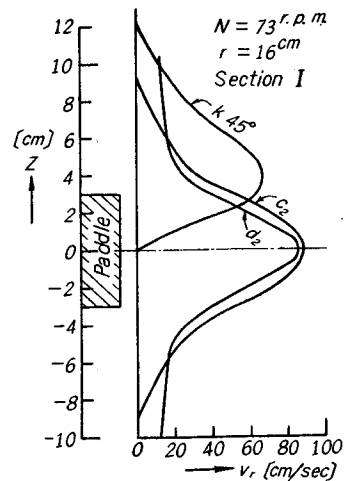
Fig. 14. Radial Velocity Distribution
of Various Types of Impellers.

for various types of impellers under the same fully-baffled condition. The curve denoted $k_{45°}$ shows the result for an 8–pitched–blade paddle having 45° blade angles (refer to **Table 1**). There is no longer a plane symmetry in the flow pattern with respect to the rotation plane of the impeller.

Values of q_1 and q_2 obtained by the processes mentioned above are shown in **Table 2.** The ratio of the circulation flow rate q_2 to the discharge flow rate q_1 are nearly constant and equal to 1.8 with little difference with the types of impellers. This value is nearly equal to that of 1.9 in the case of the non-baffled condition. Consequently, there is no great error in saying that the value of the ratio q_2/q_1 is almost 1.8~2 whether the baffle plates are used or not.

Table 2. Discharge Flow Rate and Circulation Rate.

Impeller		Discharging performance					
Symbol	Type	$[\text{r.p.m.}]$ N	$\left[\dfrac{\text{liters}}{\text{sec}}\right]$ q_1	$\left[\dfrac{\text{liters}}{\text{sec}}\right]$ q_2	$[\text{—}]$ Nq_1	$[\text{—}]$ Nq_2	$[\text{—}]$ $q_2/q_1=Nq_2/Nq_1$
c_2	8-Flat-Blade Paddle	73	44	75	1.34	2.28	1.7
d_2	8-Retreated-Blade Paddle	73	39	72	1.20	2.20	1.85
g	8-Blade-Arrow-Head Turbine	71	26.5	46.5	0.83	1.46	1.75
j	8-Blade-Brumagin-Type Impeller	72	25	44	0.78	1.36	1.75

Mean Value of $q_2/q_1 \fallingdotseq 1.8$.

Now, for the purpose of comparisons of the discharging efficiency of various impellers, the ratio of the power number $N_{P_B}=(P_B \cdot g_c/\rho n^3 d^5)$ and the coefficient of discharge N_{q_1}, (N_{P_B}/N_{q_1}), is adopted, as in the previous report, where P_B is the power consumption of the impeller under the fully-baffled condition. The performance data of various types of impellers; N_{P_B}, N_{q_1} and N_{P_B}/N_{q_1} are shown in **Table 3**, together

Table 3. Discharging Performance of Various Impellers.

Impeller		Non-Baffle				Baffled			
Symbol	Type	N_P	Nq_1	N_P/Nq_1	Re	N_{P_B}	Nq_1	N_{P_B}/Nq_1	Re
c_2	8-Flat-Blade Paddle	0.95	0.34	2.8	1×10^5	9.5	1.34	7.1	1.3×10^5
d_2	8-Retreated-Blade Paddle	0.71	0.43	1.7	"	3.8	1.20	3.2	"
g	8-Blade-Arrow-Head Turbine	0.95	0.26	3.7	"	7.7	0.83	9.3	1×10^5
j	8-Blade-Brumagin-Type Impeller	0.44	0.34	1.3	"	1.05	0.78	1.3	"
$k_{45°}$	8-Pitched-Blade Paddle	0.72	0.31	2.3	"	2.8	0.87	3.2	1.3×10^5
p_1	8-Flat-Blade Paddle	2.17	1.23	1.8	0.37×10^5	14.2	2.9	4.9	0.76×10^5

with the values of non-baffled condition for the purpose of comparison.

Referring to this Table, let the values of N_{P_B}/N_{q_1} and N_P/N_{q_1} be compared.

(i) There is a trend that the impellers having an excellent discharging performance without baffle-plates also show an excellent performance under the baffled-condition.

(ii) Insertion of flat-plate-baffles as those used commonly brings about a considerable increase (by 2~4 times) in discharging capacity N_{q_1} (also, circulating capacity N_{q_2}), but at the same time, the power consumption is greatly increased. Therefore, the discharging efficiency (also the circulation efficiency) is lowered considerably.

3) Energy Balance in the Neighbourhood of the Impellers.

An energy balance may be taken on the momentum transfer accompanied by

liquid flow in the neighbourhood of the impeller as mentioned in the previous report.

The amount of energy going out per unit time from the cylindrical section enclosing the impeller inside (as shown by ABCD in **Fig. 12**) (P_0) can be expressed as follows;

$$P_0 = \frac{\rho}{g_c} 2\pi r_s \int_0^{Z_s} v_r V^2 dz + 4\pi r_s \int_0^{Z_s} v_r p dz \qquad (5)$$

where p is the static pressure acting on the cylindrical boundary surface as shown in **Fig. 5**. Potential energy is omitted, because it cancels out. The amount of energy retuning to the impeller per unit time from the cylindrical boundary (P_i) is

$$P_i = \frac{\rho}{g_c} 2\pi \int_0^{r_s} v_z r V^2 dr + 4\pi \int_0^{r_s} v_z r p dr. \qquad (6)$$

As in the previous report, taking a cylindrical section of 32 cm in diameter and 12 cm in height, the liquid volume corresponds only to 6% of the total liquid volume. Taking up the input and output energy per unit time in this cylindrical section, the following relations are written:

$$\left.\begin{aligned} N_{P_B} &= \frac{[\text{Power consumption by impellers}]}{\rho n^3 d^5 / g_c} \\[4pt] N_{P_0} &= \frac{\left[\begin{array}{l}\text{The amount of energy going out per unit time from the}\\ \text{cylindrical section as shown in Fig. 12}\end{array}\right]}{\rho n^3 d^5 / g_c} \\[4pt] N_{P_i} &= \frac{\left[\begin{array}{l}\text{The amount of energy returning to the impeller per unit}\\ \text{time from the cylindrical boundary as shown in Fig. 12}\end{array}\right]}{\rho n^3 d^5 / g_c} \\[4pt] \varDelta N_P = N_{P_0} - N_{P_i} &= \frac{\left[\begin{array}{l}\text{Power consumption by the liquid outside the}\\ \text{cylinrical section as shown in Fig. 12}\end{array}\right]}{\rho n^3 d^5 / g_c} \\[4pt] N_{P_{\text{imp}}} = N_{P_B} - \varDelta N_P &= \frac{\left[\begin{array}{l}\text{Power consumption by the liquid inside the}\\ \text{cylindrical section as shown in Fig. 12}\end{array}\right]}{\rho n^3 d^5 / g_c}. \end{aligned}\right\} \qquad (7)$$

Referring to the 8-flat-blade paddle (c_2), these values are calculated and compared with those for the non-beffled condition in **Table 4**. These data are not accurate enough, but the authors can make an approximate energy balance in the agitation

Table 4. Energy Balance in the Neighbourhood of Impellers.
$D=58.5$ cm, $H=D$, $H_p=H/2$
Impeller used; (c_2) 8-Flat-Blade Paddle

Condition	N_P	N_{P_0}	N_{P_i}	$\varDelta N_P$	$N_{P_{imp}}$	$\dfrac{N_{P_{imp}}}{N_P} \times 100$
Non-Baffled Conditions	0.95	2.4	2.05	0.35	0.60	63%
Fully-Baffled Condition	9.5	11.2	3.0	8.2	1.3	14%

vessel.   As already mentioned in the previous report, more than one half of the power is consumed by the turbulence in the vicinity of the impeller in the case of the non-baffled condition, but this trend differs appreciably in the case of the baffled condition. That is, the distribution of the energy consumed in the liquid is considerably unified This is caused by the generation of strong cylindrical eddies as shown in **Fig. 11,** and coincides with the fact that a uniformity in stream-line distribution is attained as shown in **Fig. 9.**

IV. Conclusions

In continuation with the previous report, the flow pattern of liquid flow in an agitated vessel under a fully-baffled condition was studied and the circulating performance of the impellers was compared.

In conclusion, by the insertion of flat-plate baffles,

i)   The circumferential flow of liquid is impeded and the vertical circulation is considerably increased.

ii)   Both the distribution of the stream-line in the vertical direction and the energy consumption in the liquid are considerably unified.

iii)   However, the circulation efficiency is lowered, because the increase in the power consumption of the impeller is disproportionately greater.

iv)   There is a trend that the impellers having an excellent discharging performance in a non-baffled condition show an excellent performance in the baffled condition.

In addition, it seems probable that the circulation performance of agitators can be improved considerably by modifications of the baffle-plates.

Nomenclature

b	: Width of impeller blades	[cm]
D	: Tank diameter	[cm]
d	: Impeller diameter	[cm]
g_c	: Gravitational conversion factor	[g·cm/G·sec²]
H	: Liquid depth	[cm]
H_p	: Height of the impeller from the tank bottom	[cm]
N_{P_B}	$= P_B \cdot g_c / \rho n^3 d^5$: Power number	[——]
N_{q_1}	$= q_1/n d^3$: Coefficient of discharge	[——]
N_{q_2}	$= q_2/n d^3$: Chefficient of circulation	[——]
N_{P0}	$=$ [The amount of energy going out per unit time from the cylindrical section as shown in Fig. 12] $\div [\rho n^3 d^5/g_c]$	[——]
N_{P_i}	$=$ [The amount of energy returning to the impeller per unit time from the cylindrical boundary as shown in Fig. 12] $\div [\rho n^3 d^5/g_c]$	[——]

$\Delta N_P \quad = N_{P_0} - N_{P_i} = $ [Power consumption by the liquid outside the cylindrical section as shown in Fig. 12] $\div [\rho n^3 d^5/g_c]$ [——]

$N_{P_{imp}} = N_{P_B} - \Delta N_P = $ [Power consumption by the liquid inside the cylindrical section as shown in Fig. 12 (i.e. Power consumption in the neighbourhood of the impeller)] $\div [\rho n^3 d^5/g_c]$ [——]

N : Impeller speed in r.p.m.   [1/min.]

n : Impeller speed in r.p.s.   [1/sec.]

n_B : Number of baffle-plates   [——]

n_p : Number of impeller blades   [——]

P_B : Power consumption of impeller in fully-baffled condition   [G·cm/sec.]

P : Static pressure in liquid   [G/cm²] or [cm Aq]

q_1 : Discharge flow rate from the tip of the impeller blades

                                           [c.c/sec] or [liters/sec]

q_2 : Flow rate due to circulation   [c.c/sec] or [liters/sec]

q_{1x} : Discharge flow rate defined by Eq. (3) concerning vertical section "x"   [c.c/sec] or [liters/sec]

q_{2x} : Circulation flow rate defined by Eq. (4) concerning vertical section "x"   [c.c/sec] or [liters/sec]

r : Radial distance from the agitator axis   [cm]

V : Resultant velocity of liquid   [cm/sec]

v_t : Circumferential component of liquid velocity   [cm/sec]

v_r : Radial component of liquid velocity   [cm/sec]

v_z : Vertical component of liquid velocity   [cm/sec]

v : Resultant velocity of liquid in $r-z$ plane   [cm/sec]

w_B : Width of baffle-plates   [cm]

z : Height from the middle of liquid depth   [cm]

$\varphi',\ \theta'$: Angles determining the flow direction (refer to Fig. 2 (c))   [——]

References

1) S. Nagata, K. Yamamoto and M. Ujihara; THIS MEMOIRS, 20, 336 (1958).
2) S. Nagata, T. Yokoyama and H. Maeda; Chem. Eng. (Japan), 23 582 (1956).
3) J. P. Sachs and J. H. Rushton; Chem. Eng. Prog., 50 597 (1954).